Molybdenum Sulfide Nanoparticles in Block Copolymer Micelles: Synthesis and Tribological Properties

Tatiana P. Loginova,[†] Yurii A. Kabachii,[†] Stanislav N. Sidorov,[†] Denis N. Zhirov,[†] Peter M. Valetsky,[†] Marina G. Ezernitskaya,[†] Lidia V. Dybrovina,[†] Tatiana P. Bragina,[†] Olga L. Lependina,[†] Barry Stein,[‡] and Lyudmila M. Bronstein*[,†,§]

A.N. Nesmeyanov Institute of Organoelement Compounds, Moscow 117813, Russia, and Departments of Chemistry and Biology, Indiana University, Bloomington, Indiana 47405

Received January 19, 2004. Revised Manuscript Received March 30, 2004

Synthesis of polystyrene-*block*-polybutadiene (PS-*b*-PB) and polystyrene-*block*-polyisobutylene (PS-*b*-PIB) micelles filled with MoS_x nanoparticles was carried out in a one-pot procedure in heptane using complexation with $Mo(CO)_6$ followed by interaction with H_2S. The structure and composition of Mo carbonyl complexes and MoS_x-containing micelles were studied using FTIR, static light scattering, turbidimetry, and transmission electron microscopy. By varying the reaction atmosphere (argon or CO) during interaction with $Mo(CO)_6$, the location of MoS_x species obtained after sulfiding was tailored. Carrying out complexation with PS-*b*-PB in CO, which is also a reaction product, prevents complexation in the PS micelle core, thus providing location of Mo species only in the PB corona. Antifrictional tests show that this location leads to better tribological performance: lower friction coefficient or higher critical load (at which the friction coefficient is measured). When MoS_x species are located in the PS core (complexation with $Mo(CO)_6$ was carried out in argon atmosphere), low density of the micelles in the case of PS-*b*-PIB block copolymer with a short PS block provides much better antifrictional performance than those with the dense PS-*b*-PB micelles.

Introduction

For a number of years block copolymer micelles in selective solvents were used as nanoreactors for metal, metal oxide, and metal chalcogenide nanoparticle formation,[1−7] because block copolymers, similarly to surfactant micelles, ensure confinement for nanoparticle growth. Unlike surfactant micelles, block copolymers have important advantages: they can form free-standing films or thin films on flat or curved surfaces and other articles of interest. Block copolymer micelles filled with nanoparticles were studied in numerous catalytic reactions,[8−12] as magnetic[7,13,14] and optical[15,16] materials, for nanolithography,[17] and in biological and pharmaceutical applications.[18] To the best of our knowledge, nanoparticle-filled block copolymer micelles were not considered as additives to lubricating oils to improve their tribological properties, although oil-soluble polymers, random and even block copolymers, were widely used as antiwear modifiers. Examples are polyvinyl ether (PVE),[19] polyethyelene (PE),[20] polyisobutylene (PIB),[21] poly(alkyl methacrylates) (PMA),[22] ethylene−

* To whom correspondence should be addressed. E-mail: lybronst@indiana.edu.
[†] A.N. Nesmeyanov Institute of Organoelement Compounds.
[‡] Department of Biology, Indiana University.
[§] Department of Chemistry, Indiana University.

(1) Antonietti, M.; Henz, S. *Nachr. Chem: Technol. Lab.* **1992**, *40*, 308.
(2) Moffitt, M.; McMahon, L.; Pessel, V.; Eisenberg, A. *Chem. Mater.* **1995**, *7*, 1185.
(3) Antonietti, M.; Wenz, E.; Bronstein, L.; Seregina, M. *Adv. Mater.* **1995**, *7*, 1000.
(4) Spatz, J. P.; Roescher, A.; Möller, M. *Adv. Mater.* **1996**, *8*, 337.
(5) Underhill, R. S.; Liu, G. *Chem. Mater.* **2000**, *12*, 2082.
(6) Moffitt, M.; Vali, H.; Eisenberg, A. *Chem. Mater.* **1998**, *10*, 1021.
(7) Rutnakornpituk, M.; Thompson, M. S.; Harris, L. A.; Farmer, K. E.; Esker, A. R.; Riffle, J. S.; Connolly, J.; St. Pierre, T. G. *Polymer* **2002**, *43*, 2337.
(8) Seregina, M. V.; Bronstein, L. M.; Platonova, O. A.; Chernyshov, D. M.; Valetsky, P. M.; Hartmann, J.; Wenz, E.; Antonietti, M. *Chem. Mater.* **1997**, *9*, 923.
(9) Bronstein, L. M.; Chernyshov, D. M.; Volkov, I. O.; Ezernitskaya, M. G.; Valetsky, P. M.; Matveeva, V. G.; Sulman, E. M. *J. Catal.* **2000**, *196*, 302.
(10) Klingelhöfer, S.; Heitz, W.; Greiner, A.; Oestreich, S.; Förster, S.; Antonietti, M. *J. Am. Chem. Soc.* **1997**, *119*, 10116.
(11) Mayer, A. B. R.; Mark, J. E. *Colloid Polym. Sci.* **1997**, *275*, 333.
(12) Jaramillo, T. F.; Baeck, S.-H.; Cuenya, B. R.; McFarland, E. W. *J. Am. Chem. Soc.* **2003**, *125*, 7148.
(13) Platonova, O. A.; Bronstein, L. M.; Solodovnikov, S. P.; Yanovskaya, I. M.; Obolonkova, E. S.; Valetsky, P. M.; Wenz, E.; Antonietti, M. *Colloid Polym. Sci.* **1997**, *275*, 426.
(14) Diana, F. S.; Lee, S.-H.; Petroff, P. M.; Kramer, E. J. *Nano Lett.* **2003**, *3*, 891.
(15) Kane, R. S.; Cohen, R. E.; Silbey, R. *Chem. Mater.* **1999**, *11*, 90.
(16) Leppert, V. J.; Murali, A. K.; Risbud, S. H.; Stender, M.; Power, P. P.; Nelson, C.; Banerjee, P.; Mayes, A. M. *Philos. Mag. B* **2002**, *82*, 1047.
(17) Spatz, J. P.; Herzog, T.; Mössmer, S.; Ziemann, P.; Möller, M. *Adv. Mater.* **1999**, *11*, 149.
(18) Otsuka, H.; Nagasaki, Y.; Kataoka, K. *Adv. Drug Deliv. Rev.* **2003**, *55*, 403.
(19) Ciantar, C.; Hadfield, M.; Swallow, A.; Smith, A. *Wear* **2000**, *241*, 53.
(20) Bercea, M.; Bercea, I.; Olaru, D.; Nelias, D. *Tribol. Trans.* **1999**, *42*, 851.
(21) Guerret-Piecourt, C.; Grossiord, C.; Le Mogne, T.; Martin, J. M.; Palermo, T. *Surf. Interface Anal.* **2000**, *30*, 646.
(22) Keromest, C.; Durand, J.-P.; Born, M.; Gateau, P.; Tessier, M.; Marechal, E. *Lubr. Sci.* **1998**, *10*, 179.

10.1021/cm040147f CCC: $27.50 © 2004 American Chemical Society
Published on Web 05/20/2004

propylene copolymers,[22] hydrogenated polyisoprene-*block*-polybutadienes,[23] etc. On the other hand, oil-soluble molybdenum compounds such as dithiocarbamates (DTC) and dithiophosphates (DTP) are commonly used as additives to lubricating oils, imparting both antifrictional and antiwear properties.[24−29] It is speculated that good tribological performance of these compounds is caused by in situ formation of MoS_x species from the corresponding complexes. MoS_2 fullerene-like nanoparticles showed excellent tribological properties in solid compositions.[30−32] Recently, improved tribological properties were reported for surfactant-stabilized amorphous MoS_3 nanoparticles.[33]

We believe that Mo−sulfide nanoparticles synthesized in an oil-soluble polymer environment can be promising for achieving improved tribological properties of lubricating oils. In these systems two problems would be addressed: Mo−sulfide nanoparticles would impart antifrictional properties to lubricating oils, while block copolymers (polymeric dispersants) would improve antiwear properties. However, recent attempts to combine modified PIB and MoDTP showed a decrease of MoDTP performance as an antifriction additive.[21] In this paper we report the synthesis of Mo−sulfide nanoparticles using Mo carbonyl precursor complexes and gaseous H_2S within two types of block copolymer micelles, polystyrene-*block*-polybutadiene (PS-*b*-PB) and polystyrene-*block*-polyisobutylene (PS-*b*-PIB), in heptane as a selective solvent. The structure of MoS_x-filled block copolymer micelles and their tribological properties are described.

Experimental Procedures

Materials. $Mo(CO)_6$ and P_2S_5 were purchased from Aldrich and used as received. Heptane (Aldrich) was distilled over KOH.

Diblock PS-*b*-PB copolymer, synthesized by anionic polymerization, was obtained from Max Planck Institute of Colloids and Interfaces, Golm, Germany.[34] This block copolymer contains 85% PS and 15 wt % PB with 89% of 1,2 units and is characterized by M_w = 20 000 (from static light scattering (SLS) data; see method description below). Diblock PS-*b*-PIB copolymer containing chlorine end groups was synthesized using living carbocationic polymerization[35] at −80 °C in a 60:40 mixture of *n*-hexane/methylene chloride as a solvent. Polymerization was stopped by addition of concentrated HCl. 2-Phenyl-2-chloropropane[36] was used as an initiator. The PS-*b*-PIB copolymer sample contained 11 wt. % PS, M_w = 15 600 (by SLS).

Synthesis. Molybdenum carbonyl complexes in block copolymers were synthesized by UV irradiation (Hg lamp) of micellar block copolymer solutions in heptane in the presence of $Mo(CO)_6$. In a typical experiment, a double-jacketed quartz reactor equipped with a magnetic stir bar and a gas inlet was charged with 0.073 g (0.28 mmol) of $Mo(CO)_6$ and 30 mL of PS-*b*-PB solution in heptane with a concentration of 10 g/L (0.3 g copolymer containing 0.83 mmol of PB). Then the reactor was purged with argon or CO for 10 min, cooled to 20 °C, and UV irradiated under stirring for the reaction time. For PS-*b*-PIB, the amount of $Mo(CO)_6$ was decreased to 0.015 g (0.057 mmol). Afterward, the solution was precipitated with methanol, and the precipitate was isolated by filtration and dried in a vacuum oven overnight at 50 °C.

MoS_x species in the block copolymer micelles were obtained by treating the Mo carbonyl block copolymer solutions with H_2S under reaction temperature for 6−8 h. H_2S was obtained by reaction of P_2S_5 with water and further purified by purging it through a column filled with dried $CaCl_2$. For elemental analysis examination, the solvent was removed from the reaction solution by evaporation and the solid residue was dried overnight in a vacuum oven at 50 °C.

The following general notations have been used. PS-*b*-PB−$Mo(CO)_x$ stands for Mo carbonyl complexes formed in PS-*b*-PB micelles in CO (PS-*b*-PB−$Mo(CO)_x$-CO) or argon (PS-*b*-PB−$Mo(CO)_x$-argon) atmospheres. PS-*b*-PIB−$Mo(CO)_3$ stands for arene Mo tricarbonyl complexes in PS-*b*-PIB.

For tribological tests, the required amount of solution containing MoS_x-filled block copolymer micelles (to provide a Mo content of 500 ppm) was mixed with mineral oil. Heptane was removed first using a rotary evaporator at 40 °C at 16 mBar for 30 min and then using an oil pump at 0.6 mBar for 12 h.

Characterization. FTIR spectra were recorded using Nicolet FTIR in the range 4000−100 cm^{-1} with 2 cm^{-1} resolution. The samples were prepared as films on KBr windows or as KBr pellets.

Molybdenum content in the samples was assessed by X-ray fluorescence (XRF) measurements performed with a Zeiss Jena VRA-30 spectrometer. Analyses were based on the Co Kα line and a series of standards prepared by mixing 1 g of polystyrene with 10−20 mg of standard compounds. Sulfur content was assessed via burning the samples with oxygen in the closed flask followed by addition of water and titration with 0.01 M $Ba(CH_3COO)_2$ solution.[37]

Examination of molecular weights (MW) was performed by SLS measurements with the Fica-50 goniodiffusometer using vertically polarized light of 546-nm wavelength, in the angle interval 30−150° at 25 °C by a standard procedure.[38] SLS allows assessment of the weight-average molecular weight of polymers (M_w) and virial coefficients.[38] The instrument was calibrated using benzene as a standard. Prior to the measurements, solutions were filtered through Millipore filters with pore diameter of 0.22 μM. The specific partial volume $\bar{v}$ and solvent density ρ_0 were measured by pycnometry (T = 25 ± 0.05 °C). Before measurement the pycnometer was calibrated with Hg.

Micelle sizes were examined by the spectra turbidity method (turbidimetry) using a photoelectrical colorimeter FEK-56M (Russia) equipped with a high-pressure mercury-quartz lamp (DPK-120).[39,40] Using a number of filters, the turbidity τ and optical density D were obtained. In the limited range of the wavelengths (λ = 315−600 nm), spectral dependence of the turbidity can be expressed using the Angstrom equation

(23) Coolbaugh, T. S.; Loveless, F. C.; Marlin, J. E., II; Matthews, D. N. PCT Int. Appl. 20010118, 2001.
(24) Muraki, M.; Yanagi, Y.; Sakaguchi, K. *Tribol. Int.* **1997**, *30* (1), 69−75.
(25) Yamamoto, Y.; Gondo, S. *Tribol. Trans.* **1989**, *32*, 251.
(26) Leslie, W. L.; Root, J. C. U.S. Patent 6,376,432, 2002.
(27) Watanabe, A.; Kunugi, T.; Kumakura, A.; Sanze, K.; Hasegawa, S. JP 2001131570, 2001.
(28) Shea, T. M.; Stipanovic, A. J. *Tribology Lett.* **2002**, *12*, 13.
(29) Neville, A.; Kollia-Rafailidi, V. *Wear* **2002**, *252*, 227.
(30) Chhowalla, M.; Amaratunga, G. A. J. *Nature* **2000**, *407* (6801), 164.
(31) Feldman, Y.; Zak, A.; Popovitz-Biro, R.; Tenne, R. *Solid State Sci.* **2000**, *2*, 663.
(32) Rapoport, L.; Leshchinsky, V.; Volovik, Y.; Lvovsky, M.; Nepomnyashchy, O.; Feldman, Y.; Popovitz-Biro, R.; Tenne, R. *Surf. Coat. Technol.* **2003**, *163−164*, 405.
(33) Parenago, O. P.; Bakunin, V. N.; Kuz'mina, G. N.; Suslov, A. Y.; Vedeneeva, L. M. *Dokl. Chem.* **2002**, *383*, 86.
(34) Antonietti, M.; Foerster, S.; Hartmann, J.; Oestreich, S. *Macromolecules* **1996**, *29*, 3800.
(35) Storey, R. F.; Chisholm, B. J. *Macromolecules* **1993**, *26*, 6727.
(36) Kharasch M. S.; Brown, H. C. *J. Am. Chem. Soc.* **1939**, *61*, 2142.
(37) Gilman, N. E.; Trentieva, E. A.; Shanina, T. M. *Methods of Quantitative Organic Elemental Analysis*; Khimiya: Moscow, 1987.
(38) Huglin, M. B. *Light Scattering from Polymer Solutions*; Academic Press: London-New York, 1972.
(39) Heller, W.; Bhatnagar, H. L.; Nakagaki, M. *J. Chem. Phys.* **1962**, *36*, 1163.
(40) Heller, W.; Pangonis, W. J. *J. Chem. Phys.* **1957**, *26*.

$$\tau = A \cdot \lambda^{-n}$$

where n is the wave exponent that is the function of relative particle size, α, and relative particle refractive index, m; A is the constant obtained from the logarithmic dependence between τ and λ. To find n, experimental data on τ and D were plotted in double logarithmic coordinates and n was found as the slope. Using correlations of n and M_n in a wide range of α and m, particle radius was calculated

$$r_w = \frac{\alpha \times \lambda_{av}}{2\pi\mu_1}$$

where μ_1 is the refractive index of the dispersion medium and λ_{av} is the average wavelength found from the equation

$$\lambda_{av} = \sqrt{\lambda_{max} \times \lambda_{min}}$$

Specimens for transmission electron microscopy (TEM) were prepared by placing a drop of solution onto a carbon-coated copper grid. Images were acquired at accelerating voltages of 60 kV on a JEOL JEM1010 microscope.

X-ray powder diffraction (XRD) measurements were performed on a Rigaku D/max-RC X-ray diffractometer operating at 12-kV Cu *K*α radiation.

Antifrictional tests of MoS_x-filled block copolymer micelles in mineral oil (Exxon 100 LP) were performed using a ball-on-disk tribometer SRV (Optimol, Germany) with 1-mm amplitude and frequency of 20 GHz. The friction coefficient was measured at a constant temperature under the increasing load. The load corresponding to a sharp increase of a friction coefficient was taken as a critical load L_c. Antiwear tests were carried out using a standard four-ball wear test machine (Russia) with a ball diameter of 14.7 mm. Wear index was estimated as a diameter of the wear spot developed in 1 h at 20 °C under a permanent load of 196 N.

Results and Discussion

Successful synthesis of crystalline MoS_2 nanoparticles in inverse surfactant micelles using Mo−halide as a Mo precursor was reported in refs 41 and 42, but this path results also in HCl (as a side product) residing in the micelles that is undesirable for lubricating oil compositions. In another procedure,[43] amorphous MoS_x nanoparticles with diameters of 3−10 nm were synthesized in AOT (bis(2-ethylhexyl)sulfosuccinate sodium salt)/water/*n*-heptane microemulsions using ammonium tetrathiomolybdate as the Mo precursor and again acidic solution (sulfuric acid) to cause tetrathiomolybdate decomposition. In contrast, interaction of $Mo(CO)_6$ with H_2S, resulting in MoS_x nanoparticles,[44−46] produces only easily removable gases (H_2 and CO) as side products so block copolymer solution (and lubricating oil afterward) should be free from any undesirable side products. Because MoS_x nanoparticles can be synthesized by interaction of $Mo(CO)_6$ with H_2S, we expected that substituted Mo carbonyl complexes (with double bonds or benzene rings), incorporated in block copolymer micelles, will also give MoS_x species when subjected to H_2S.

Scheme 1. Reaction Pathways for PB and PS Repeating Units under UV-irradiation of $Mo(CO)_6$ Reaction Solutions

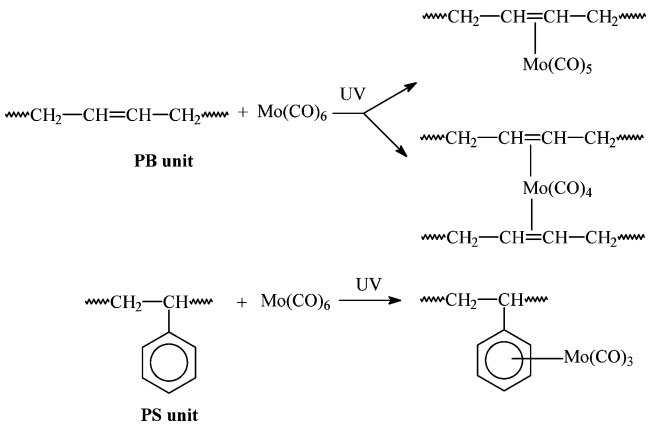

Formation of Mo Carbonyl Complexes in PS-*b*-PB. *FTIR Study.* Mo carbonyl complexes of general formula $[Mo(CO)_{6-n}L_n]$ where L is an alkene, can be synthesized from $Mo(CO)_6$ and the corresponding alkenes at elevated temperatures or with UV irradiation. In so doing, the complex structure depends on the alkene structure and reaction conditions:[47−50] one, two, or even four carbonyl ligands can be substituted with double bonds (Scheme 1). Compounds containing benzene rings also give complexes with Mo hexacarbonyl (normally under heating) forming π-arene Mo tricarbonyl structure.[50,51]

Although π-alkene and π-arene Mo carbonyl complexes of different structure have been known for more than 40 years, similar complexes with PB were hardly ever systematically studied: a few references[52,53] mention formation of Mo carbonyl complexes with one or two double bonds of PB or other polymers containing double bonds. Polystyrenes containing π-arene Mo tricarbonyl complexes were prepared from triacetonitrile tricarbonyl Mo complexes and PS,[54] but not directly from $Mo(CO)_6$. Thus, for block copolymer micelles in heptane, the particular conditions of complexation in the PS core or in the PB corona were not known and required clarification. We expected that first of all (and mainly) complexation with $Mo(CO)_6$ would occur in the PB corona as the double bonds are more prone to complexation with $Mo(CO)_6$ and more easily available in the micellar solution. This would address the desired application: location of Mo species in the micelle corona

(41) Wilcoxon, J. P.; Samara, G. A. *Phys. Rev. B* **1995**, *51*, 7299.
(42) Thurston, T. R.; Wilcoxon, J. P. *J. Phys. Chem. B* **1999**, *103*, 11.
(43) Marchand, K. E.; Tarret, M.; Lechaire, J. P.; Normand, L.; Kasztelan, S.; Cseri, T. *Colloids Surf., A* **2003**, *214*, 239.
(44) Close, M. R.; Petersen, J. L.; Kugler, E. L. *Inorg. Chem.* **1999**, *38*, 1535.
(45) Rodriguez, J. A.; Dvorak, J.; Jirsak, T.; Hrbek, J. *Surf. Sci.* **2001**, *490*, 315.
(46) Okamoto, Y.; Katsuyama, H. *Ind. Eng. Chem. Res.* **1996**, *35*, 1834.
(47) Dub, M. *Organometallic Compounds*, 2nd ed.; Springer-Verlag: Berlin, 1966; Vol. 1.
(48) Green, Malcolm Leslie H. *Organometallic Compounds, The Transition Elements*, 3rd ed.; Barnes and Noble: New York, 1967; Vol. 2.
(49) Herberhold, M. *Metal Pi-Complexes*; Vol. 2: Complexes with Monoolefinic Ligands, Pt. 1: General Survey, Elsevier: New York, 1972.
(50) Wilkinson, G., Ed. *Comprehensive Organometallic Chemistry*, 1st ed.; Pergamon Press: Oxford, 1982; Vol. 3.
(51) Strohmeier, W. *Chem. Ber.* **1961**, *94*, 337.
(52) Dawans, F.; Morel, D. DE 2605247, 1976.
(53) Kalinina, E. V.; Kozyreva, N. M.; Valetskii, P. M.; Korshak, V. V. *Polybutadiene pi-complexes of Molybdenum and Tungsten*; Moscow, 1982; Deposited Doc. (VINITI 6367-82).
(54) Pittman, C. U., Jr.; Grube, P. L.; Ayers, O. E. *Pap. Meet. − Am. Chem. Soc., Div. Org. Coatings Plast. Chem.* **1971**, *31*, 325.

seems to be desirable, as it should ensure accessibility of the MoS_x particles (when particles are formed) for lubricated surfaces. On the other hand, we also considered the possible interaction of PS units with $Mo(CO)_6$ in the reaction conditions (Scheme 1).

Synthesis of MoS_x nanoparticles in PS-*b*-PB and PS-*b*-PIB micelles was carried out in a one-pot procedure using two steps: first, complexation of $Mo(CO)_6$ with block copolymer under UV irradiation (in CO or argon atmosphere) and subsequent interaction of molybdenum carbonyl complexes with H_2S. It was anticipated that a CO atmosphere should decrease the degree of carbonyl group substitution (CO is the product of complexation), thus, it should ensure formation of monosubstituted pentacarbonyl complexes within the micelle corona and thwart formation of diolefin $Mo(CO)_4$ species. The latter may lead to cross-linking between coronas of different micelles and, thus, precipitation of the block copolymer micelles. In addition, a CO atmosphere was expected to prevent formation of arene Mo carbonyl complexes in the PS core, since, in this case, three CO groups in $Mo(CO)_6$ should be replaced with one arene to form the complex.

Although PS-*b*-PB and $Mo(CO)_6$ are colorless, the reaction solutions obtained after interaction of PS-*b*-PB with $Mo(CO)_6$ in a CO atmosphere are light brown. After sulfiding the solution, it darkened to brown. In argon, the reaction solutions containing carbonyl complexes are brown, and sulfiding led to dark brown solutions. FTIR spectra of all PS-*b*-PB−$Mo(CO)_x$ solutions after UV irradiation contained a weak broad band at 1983 cm^{-1} assigned to nonreacted $Mo(CO)_6$ (this band is present in the FTIR spectrum of the $Mo(CO)_6$ solution in heptane), but this band was subtracted from the spectra to facilitate their interpretation. From Figure 1, one can see that the FTIR spectra of the Mo carbonyl complexes derived from PS-*b*-PB and obtained using CO or argon atmosphere are dissimilar, although both contain a number of bands in the CO stretching region. To clarify the structure of the complexes, PS and PB homopolymers were subjected to complexation with $Mo(CO)_6$ under the same conditions as those for PS-*b*-PB block copolymer.

The FTIR spectrum of the Mo-carbonyl PS prepared in argon atmosphere contains two ν(CO) bands at 1981 and 1939 cm^{-1}, the intensity and shape of which are typical for arene tricarbonyl complexes, $ArMo(CO)_3$ (see inset in Figure 1a). These frequencies are higher than those described for small arenes[55] which can be caused by polymeric nature of the ligand. When UV irradiation occurs in a CO atmosphere, *no* Mo carbonyl complexes form in PS. The FTIR spectra of the molybdenum carbonyl complexes formed in PB (both in CO and Ar) contain a number of overlapping bands in the CO stretching region, which presumably correspond to a mixture of alkene Mo carbonyl complexes with different degree of carbonyl group substitution and different alkene structure (one should remember that PB contains both 1,2- and 1,4-units the complexes of which should give different bands in FTIR spectra), but their correct assignment is difficult (inset in Figure 1b). As well established, depending on the degree of carbonyl

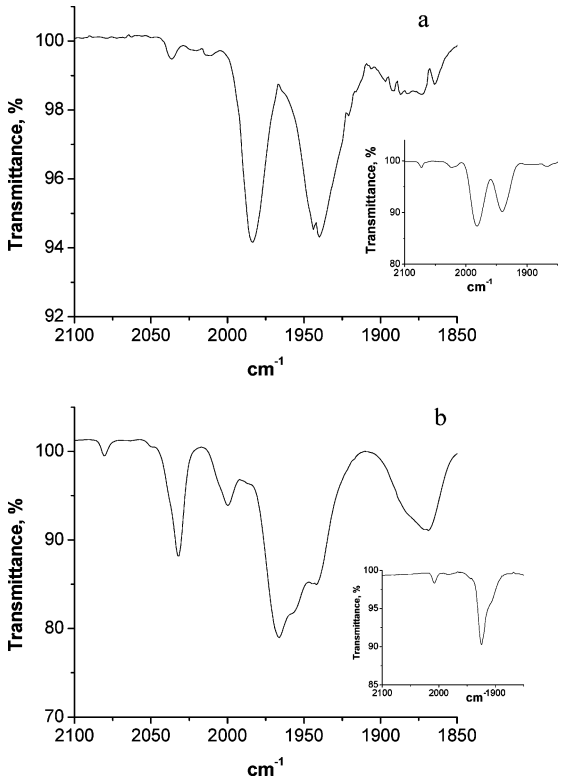

Figure 1. FTIR spectra of PS-*b*-PB−Mo-1 (a) and PS-*b*-PB−Mo-6 (b). The former sample was prepared in argon atmosphere, whereas the latter one was synthesized using CO atmosphere for 1 h. The insets in (a) and (b) show the FTIR spectra of PS and PB, respectively, containing Mo carbonyl complexes.

group substitution, complexes have different numbers of ν(CO) bands. According to previous works,[56−59] $LMo(CO)_5$ complexes with C_{4v} symmetry give three CO stretching bands, whereas $L_2Mo(CO)_4$ complexes with C_{2v} symmetry give four bands. For a mixture of penta- and tetracarbonyl complexes, some ν(CO) bands overlap; however, the bands at 2087 cm^{-1} and 2031 cm^{-1} stand separately and can be used to indicate the presence of pentacarbonyl and tetracarbonyl alkene complexes, respectively. This allows us to suggest tentative assignment of the bands for the mixtures of Mo carbonyl olefin complexes in block copolymers.

As mentioned above, interaction of $Mo(CO)_6$ with PS-*b*-PB occurs differently depending on the reaction atmosphere. The FTIR spectrum of PS-*b*-PB−$Mo(CO)_x$-argon (synthesized in argon), contains two ν(CO) bands at 1984 and 1939 cm^{-1} (Figure 1a) which exactly match the bands observed in the FTIR spectrum of PS homopolymer. This unambiguously confirms formation of arene-$Mo(CO)_3$ complexes in PS-*b*-PB block copolymer, i.e., complexation *only* in the PS core (Scheme 1). The FTIR spectrum of PS-*b*-PB−$Mo(CO)_x$-CO (obtained in a CO atmosphere) contains six bands at 2087, 2031, 1983, 1966, 1942, and 1934 cm^{-1} (Figure 1b) which can be assigned to a mixture of molybdenum penta-, tetra-,

(55) Nesmeyanov, A. N.; Krivykh, V. V.; Kaganovich, V. S.; Rybinskaya, M. I. *J. Organomet. Chem.* **1975**, *102*, 185.

(56) Stolz, I. W.; Dobson, G. R.; Sheline, R. K. *Inorg. Chem.* **1963**, *2*, 323.

(57) Fischer, E. O.; Kogler, H. P.; Kuzel, P. *Chem. Ber.* **1960**, *93*, 3006.

(58) Abel, E. W.; Bennett, M. A.; Burton, R.; Wilkinson, G. *J. Chem. Soc.* **1958**, 4559.

(59) Kraihanzel, C. S.; Cotton, F. A. *Inorg. Chem.* **1963**, *2*, 533.

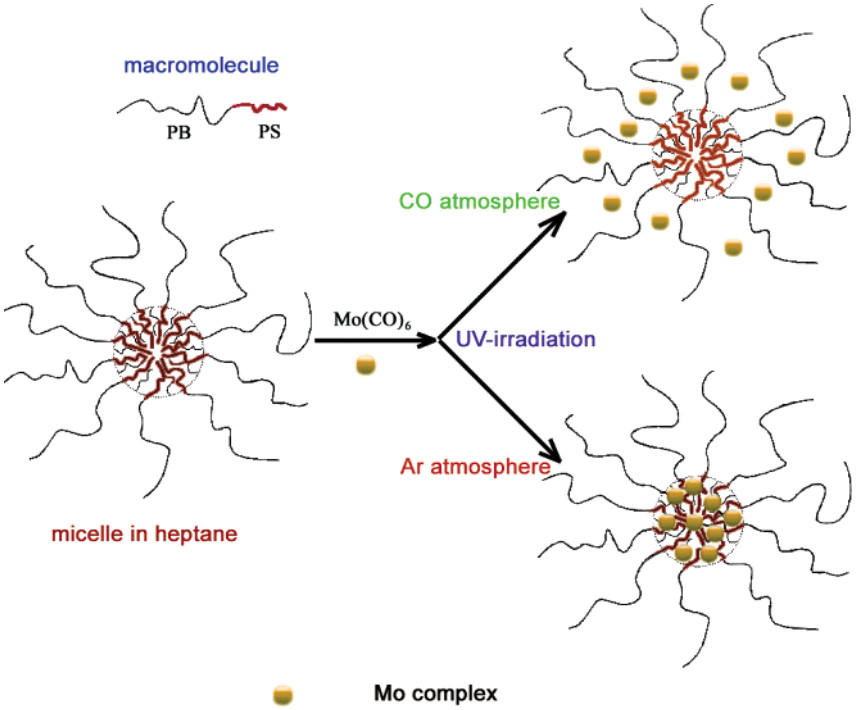

Figure 2. Complexation of Mo carbonyl species with functional groups of the PS-*b*-PB micelles depending on the reaction conditions.

and dicarbonyl complexes.[56−58] This spectrum does not match that of PB−Mo(CO)$_x$-CO due to different PB composition, but shows no bands assigned to arene-Mo-(CO)$_3$. As discussed above, *no* carbonyl complexes were obtained in the PS homopolymer in a CO atmosphere, indicating that the PS core in the PS-*b*-PB micelles should be complex-free, while complexation occurs solely in the micelle corona.

The striking difference in complexation depending on the reaction atmosphere can be explained in the following way. When CO removal is suppressed (in a CO atmosphere), arene Mo tricarbonyl complexes cannot form, as three carbonyl ligands should be replaced with one arene ring for each Mo carbonyl complex. This results in complexation solely in the micelle corona. When argon atmosphere is used, this facilitates formation of arene Mo tricarbonyl complexes. Because the fraction of PS units in this block copolymer is larger than that of PB units, the probability of complexation in the PB corona in these conditions seems to be low. We cannot completely exclude formation of π-olefin Mo carbonyl complexes in the PB corona, but their fraction should be negligible. On the basis of the FTIR data, complex formation with PS-*b*-PB is illustrated in Figure 2.

For the PS-*b*-PIB block copolymer, UV irradiation in a CO atmosphere results in the material containing *no* Mo carbonyl species (similar to PS). At the same time, UV irradiation in argon leads to the polymer whose FTIR spectrum contains two major ν(CO) bands at 1966 and 1885 cm^{-1} (PS-*b*-PIB−Mo(CO)$_3$, Figure 3). This is additional evidence that the reaction atmosphere determines the way of complexation and the location of the Mo carbonyl complexes. The positions of ν(CO) bands exactly match those described for small arene complexes.[55] Thus, when the core-forming block is short (~17 units), the "neighbor" does not influence the IR frequencies.

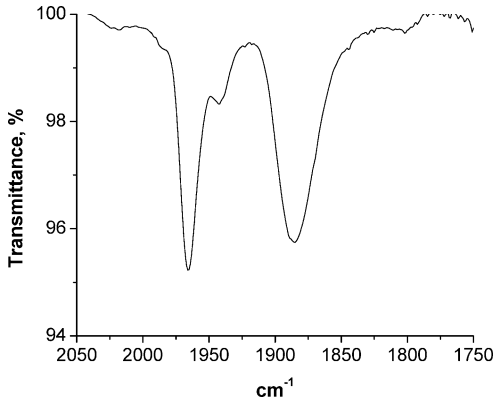

Figure 3. FTIR spectrum of PS-*b*-PIB−Mo-2 prepared in argon atmosphere for 2 h.

Table 1. Composition of Mo(CO)$_x$-filled Block Copolymers Depending on the Reaction Conditions

sample notation	reaction atmosphere	reaction time, h	Mo content, wt %[a]
PS-*b*-PB−Mo-1	Ar	1.0	2.5
PS-*b*-PB−Mo-2	Ar	1.5	4.0
PS-*b*-PB−Mo-3	Ar	2.0	5.2
PS-*b*-PB−Mo-4	Ar	4.0	6.7[b]
PS-*b*-PB−Mo-6	CO	1.0	1.8
PS-*b*-PB−Mo-7	CO	2.0	2.5
PS-*b*-PB−Mo-8	CO	2.5	3.8
PS-*b*-PB−Mo-9	CO	3.0	4.2[b]
PS-*b*-PIB−Mo-1	Ar	1.0	1.2
PS-*b*-PIB−Mo-2	Ar	2.0	3.5

[a] By elemental analysis data. [b] Samples precipitated from the reaction solutions in a few hours after reaction.

We studied the influence of the reaction atmosphere and the time of UV irradiation on the composition of Mo carbonyl-containing polymers (Table 1). An increase of irradiation time from 1 to 3 h for CO and from 1 to 4 h for argon atmosphere results in an increase of the

Table 2. Composition of Block Copolymers Containing MoS_x Species

sample notation	sulfiding temp, °C	Mo content, wt. %[a]	S content, wt. %[a]	wt. % Mo/ wt. % S
MoS_2		60	40	1.5
MoS		75	25	3.0
MoS_3		50	50	1.0
PS-*b*-PB−Mo-1-S	40	2.5	0.8	3.1
PS-*b*-PB−Mo-1-S-98	98	2.5	2.3	1.1
PS-*b*-PB−Mo-2-S	40	4.0	1.2	3.4
PS-*b*-PB−Mo-3-S	40	5.2	1.6	3.2
PS-*b*-PB−Mo-6-S	40	1.8	0.6	3.0
PS-*b*-PB−Mo-6-S-98	98	1.8	1.5	1.2
PS-*b*-PB−Mo-8-S	40	3.8	1.3	2.9
PS-*b*-PIB−Mo-2-S	98	3.5	2.5	1.4

[a] By elemental analysis data.

Table 3. Molecular and Micellar Characteristics of PS-*b*-PB and PS-*b*-PIB Block Copolymers after a Corresponding Treatment

sample notation	solvent	M_w, g/mol	$A_2 \times 10^4$, cm^3 mol/g^2	R_t, nm[a]
PS-*b*-PB	THF	20 000	11.6	52
PS-*b*-PB	chloroform	19 400	11.8	
PS-*b*-PB (2 h UV irradiation)	THF	23 500	10.0	55
PS-*b*-PB−Mo-1	THF	25 000	12.8	62
PS-*b*-PB−Mo-6	THF	50 800	1.13	61
PS-*b*-PIB	chloroform	15 600	11.0	52
PS-*b*-PIB (2 h UV irradiation)	chloroform	22 000	4.0	57
PS-*b*-PIB−Mo-2	chloroform	24 000	4.0	68

[a] In heptane solutions.

degree of complexation (Mo content increases). At the same time, at prolonged reaction times micelles precipitate in a few hours after completion of the reaction. For the polymers obtained in a CO atmosphere, this might be caused by intermicellar interactions due to a higher fraction of $Mo(CO)_4$ species at a higher degree of complexation. In the case of an argon atmosphere, when complexation occurs only within the micelle core, the "cross-linking scenario" is hardly possible. On the other hand, increase of the arene $Mo(CO)_3$ complex fraction may change micelle characteristics which would result in micelle instability. The discussion below concerning the shapes of micelles (from the TEM study) will help to confirm this supposition.

SLS Study. Influence of complexation with Mo carbonyl species on the molecular weights of block copolymers was studied using SLS. As can be seen from Table 3, molecular weights and second virial coefficients of pristine PS-*b*-PB examined in THF and chloroform are similar and the second virial coefficients are high, so both are good solvents.[60] The 2-h UV treatment of the PS-*b*-PB block copolymer solution results in a small increase of the molecular weight and a decrease of the A_2 value that reflects the formation of a small fraction of larger macromolecules[61,62] (dimers, trimers, etc.) due to double bond polymerization. After interaction with $Mo(CO)_6$ in argon resulting in the formation of arene Mo tricarbonyl complexes in the micelle cores (PS-*b*-PS−Mo-1), the molecular weight of the block copolymer changes only slightly which may reflect addition of the Mo carbonyl complexes. Because the added weight due to complexation would be about 5 wt %, this value might go unnoticed, as the accuracy of the method is also about 5%.[39] A noticeable increase of A_2 for this sample is accounted for by the presence of $Mo(CO)_3$ fragments in the polymer chain: these fragments have high affinity to THF and may lead to an increase of A_2. In comparison, the changes in molecular weight and A_2 observed for PS-*b*-PB−Mo-6 are striking. As the molecular weight more than doubles, A_2 decreases by the order of magnitude. These changes can be ascribed to formation of a significant portion of diolefin Mo tetracarbonyl complexes connecting the double bonds of two neighboring macromolecules. This may lead to branching of the macromolecules and a decrease of A_2.[62]

For PS-*b*-PIB, UV irradiation results in more considerable changes than for PS-*b*-PB: molecular weight increases and A_2 decreases more strongly. This can be caused by decomposition of 1-phenyl-chloroethyl end groups under UV irradiation with formation of 1-phenylethyl radicals. Their reactions (chain transfer, recombination, etc.) may result in partial cross-linking and formation of a branched polymer.[62] At the same time, incorporation of $Mo(CO)_3$ complexes after interaction with $Mo(CO)_6$ (PS-*b*-PIB−Mo-2) results in only a slight increase of a molecular weight (compared to the irradiated sample) which matches well to 3.5 wt % Mo. The A_2 value does not change that which can be caused by no change in interaction between chloroform and a macromolecule when a metal complex is formed.

MoS_x Nanoparticle Formation in Block Copolymer Micelles. *Composition of MoS_x Species.* MoS_x nanoparticles in the PS-*b*-PB and PS-*b*-PIB micellar solutions in heptane were obtained by interaction of block copolymer micelles containing Mo carbonyl complexes with H_2S similar to a method described elsewhere.[46] In our work, the highest reaction temperature

(60) Kalpagam, V.; Ramakrishna, R. M. *J. Polym. Sci. A* **1963**, *1*, 233.
(61) Fujita, H.; Norisuye, T. *Macromolecules* **1985**, *18*, 1637.
(62) Douglas, J. F.; Roovers, J.; Freed, K. F. *Macromolecules* **1990**, *23*, 4168.

was limited by the heptane boiling point: 98 °C, whereas in ref 46 Mo sulfide from $Mo(CO)_6$ was formed at 100 °C and higher. We studied sulfiding at different temperatures and followed the progress of reaction using FTIR spectroscopy and elemental analysis. When the sulfiding temperature was 20 °C, the PS-*b*-PB−$Mo(CO)_x$-CO sample precipitated after 8 h of H_2S treatment. The FTIR spectrum of this block copolymer sample still contained a number of ν(CO) bands, however, they differed from the bands in the spectrum of the initial Mo complex. The FTIR band at 2081 cm^{-1} associated with $Mo(CO)_5$ complexes disappeared, while bands which might be assigned to tetracarbonyl complexes of different symmetry were present in the spectrum. Clearly, the higher degree of carbonyl ligand substitution caused intermicellar interaction and precipitation. At 30−60 °C, sulfiding for 8 h resulted in total removal of the carbonyl ligands and stable PS-*b*-PB−MoS_x micellar solutions. These solutions showed an exceptional stability (for more than a year) and an excellent miscibility with mineral oil. Increase of reaction temperature to 70−98 °C led to precipitation of block copolymers from the reaction solutions that might be caused by double bond polymerization leading to intermicellar cross-linking. The composition of MoS_x species obtained in PS-*b*-PB micelles is presented in Table 2. One can see that when sulfiding temperature is 40 °C (similar results are obtained in the temperature range 30−60 °C), the PS-*b*-PB block copolymer samples containing either alkene or arene Mo carbonyl complexes give molybdenum sulfide species, the composition of which is close to Mo/S =1:1. This can be caused by coexistence of Mo(0) species surrounded with MoS_2.[45] Increase of sulfiding temperature to 98 °C (for PS-*b*-PB−Mo-1 and PS-*b*-PB−Mo-6) leads to a significant increase of sulfur in the sample, which becomes close to that for the formula MoS_3. In the PS-*b*-PIB−Mo-2 sample, sulfiding at 98 °C results in the composition matching that of MoS_2. Thus, one can conclude that by varying the sulfiding temperature, one can vary the composition of the MoS_x species, while the structure of the preceding Mo carbonyl complex does not affect the MoS_x composition. Unlike PS-*b*-PB block copolymer, 98 °C sulfiding of PS-*b*-PIB−$Mo(CO)_3$ sample does not cause precipitation of the block copolymer as the PIB block is chemically stable in these conditions.

Turbidity Spectra Measurements. Micellar behavior of block copolymers was studied in heptane, which is a selective solvent for these block copolymers (a good solvent only for PB and PIB blocks). According to turbidity spectra measurements, the radius of the PS-*b*-PB micelles is 52 nm and it rises to 55 nm after 2 h UV treatment. Incorporation of metal complexes both in the core (PS-*b*-PB−Mo-1) and in the corona (PS-*b*-PB−Mo-6) results in the increase of micellar radius to 60 nm. However, the maximum calculated micelle radius for fully extended PS-*b*-PB chains is only about 33 nm. Normally, the radius of the real micelles is equal to or smaller than the length of the fully extended polymer chain. The possible cause of unrealistically high micelle radii, found by turbidimetry, lies in the formation of micellar aggregates or wormlike micelles which may strongly increase the value of the average micelle radii. To clarify that, we carried out TEM examination of the PS-*b*-PB−MoS_x samples taking into account that MoS_x species should provide a natural staining of the micelles. Another goal of TEM examination was to determine the size of MoS_x nanoparticles.

TEM Examination of MoS_x-Filled PS-b-PB and PS-b-PIB Micelles. PS-*b*-PB, containing short PB block (25.5 mol %) and larger PS block, can be assigned to a family of so-called "crew-cut" micelles whose numerous morphologies in water were well described in a number of publications.[63,64] At the same time, the PS-*b*-PIB used here, by block ratio, is similar to block copolymers forming spherical micelles.

Figure 4 shows TEM images of PS-*b*-PB−Mo-1-S and PS-*b*-PB−Mo-6-S block copolymer micelles. These samples were subjected to interaction with $Mo(CO)_6$ for 1 h in argon and CO atmospheres, respectively, followed by interaction with H_2S at 40 °C. One can see that PS-*b*-PB−Mo-1-S forms very-well-defined and dense (high-contrast) spherical micelles with prevailing diameters of 60 nm that match fairly well to double the size of fully extended block copolymer chains. Some micelles are larger and measure up to 86 nm in diameter. The larger micelles can be formed with participation of a small fraction of dimer macromolecules formed during UV irradiation. The high micelle density seen in Figure 4a is well supported by the low specific partial volume, $\bar{v}$, which is inversely related to the density of the micellar structures.[65] For PS-*b*-PB−Mo-1-S, $\bar{v}$ is 0.767, whereas for UV-irradiated PS-*b*-PB this value is 0.807. A close look at the micrograph (see inset in Figure 4a) shows that the central part of the micelle (about 38-nm diam) is darker and contains nanoparticles with diameters of about 1.5−2 nm. Micelles are prone to aggregation although they are still discrete. Apparently, these aggregates of micelles exist also in solution, which is reflected in the high values of R_t obtained from the turbidity measurements (Table 3). The PS-*b*-PB−Mo-6-S micelles are also well defined and measure about 40 nm in diameter but show signs of coalescence (pairs of micelles are fused) (Figure 4b). Larger aggregates with no clear interfaces between micelles are also seen. These observations explain the high R_t values. The PS-*b*-PB−Mo-6-S micelles are more uniformly stained with MoS_x (no dark central parts are seen) which is in good agreement with MoS_x nanoparticle formation in the micelle corona. Here, $\bar{v}$ is equal to 0.859 which is evidence of comparatively low density of the micellar structures. Coalescence of the micelles may be caused by formation of diolefin Mo tetracarbonyl complexes between two micelle coronas. In this system, nanoparticles are hardly seen so we believe that they are smaller than 1 nm. XRD patterns obtained for both MoS_x-filled block copolymer samples are featureless, i.e., they show *no* crystalline species. As reported in ref 66 MoS_2 crystallites of approximately 3 nm can be assessed in the pure MoS_2 phase, although lines in the XRD pattern are broad. In our case, either particles are amorphous

(63) Zhang, L.; Eisenberg, A. *J. Am. Chem. Soc.* **1996**, *118*, 3168.
(64) Yu, K.; Eisenberg, A. *Macromolecules* **1998**, *31*, 3509.
(65) Bronstein, L. M.; Chernyshov, D. M.; Vorontsov, E.; Timofeeva, G. I.; Dubrovina, L. V.; Valetsky, P. M.; Kazakov, S.; Khokhlov, A. R. *J. Phys. Chem. B* **2001**, *105*, 9077.
(66) Borsella, E.; Botti, S.; Cesile, M. C.; Martelli, S.; Nesterenko, A.; Zappelli, P. G. *J. Mater. Sci. Lett.* **2001**, *20*, 187.

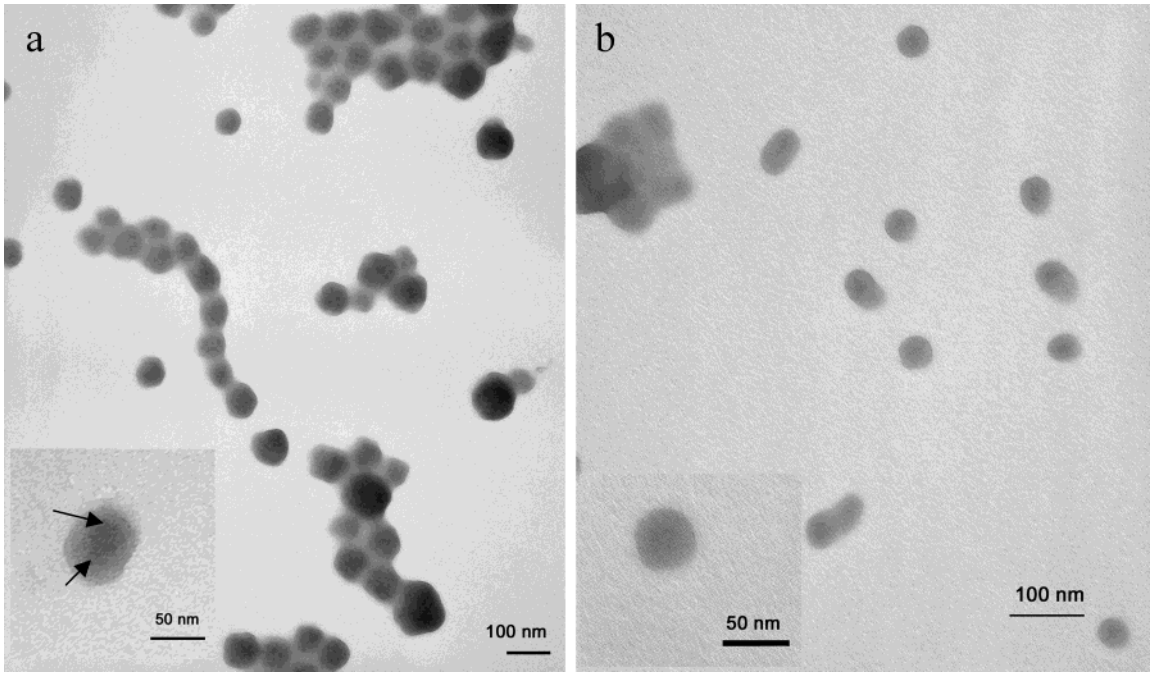

Figure 4. TEM images of PS-*b*-PB−Mo-1-S (a) and PS-*b*-PB−Mo-6-S (b). Insets show micelles at higher magnification. Both samples contain spherical micelles. Nanoparticles are shown by arrows (inset b).

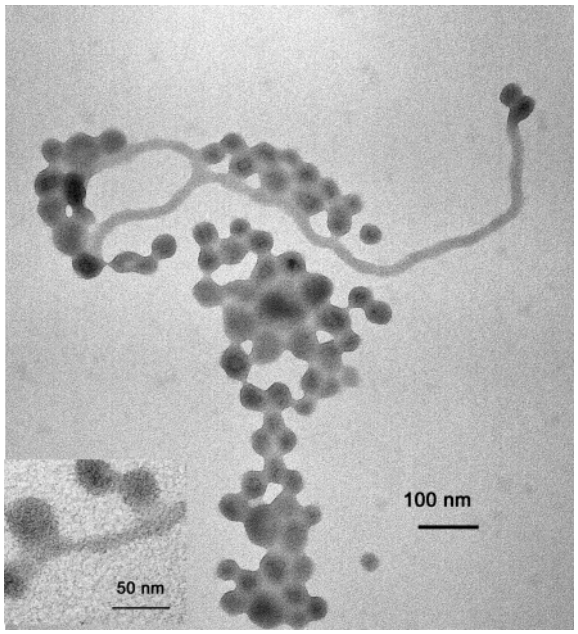

Figure 5. TEM image of PS-*b*-PB−Mo-3-S micelles. Inset shows a higher magnification image. Sample contains both spherical and wormlike micelles.

or they are too small and their volume fraction is too low to be successfully examined by XRD.

The TEM image of PS-*b*-PB−Mo-3-S (subjected to interaction with $Mo(CO)_6$ for 2 h in an argon atmosphere followed by interaction with H_2S at 40 °C) shows two types of micelles: spherical and wormlike (Figure 5). Moreover, spherical micelles are smaller than the ones for PS-*b*-PB−Mo-1-S and measure about 35−40 nm in diameter. Diameters of the giant wormlike micelles are even smaller and do not exceed 15 nm. Evidently, when the degree of complexation with $Mo(CO)_3$ species in the micelle core is higher (by a factor of 2, compared to PS-*b*-PB−Mo-1-S), the core-forming block contains more polar species which should cluster in multiplets within the hydrophobic PS phase.[67,68] The change of block copolymer morphology with increase of complexation degree with $Co_2(CO)_8$ was recently reported for PS-*b*-P2VP block copolymer.[69] Presumably, in our case, the interfacial energy between multiplets and surrounding hydrophobic PS is larger than the interfacial energy between PS core and PB corona, so the former factor will determine the micellar characteristics: decreased micelle size and formation of wormlike micelles. These huge wormlike micelles along with increased aggregation of spherical micelles can cause solution instability of the PS-*b*-PB−$Mo(CO)_3$ samples with high Mo content (PS-*b*-PB−Mo-4 precipitates in a few hours after completion of reaction).

Figure 6 presents the TEM image of the PS-*b*-PIB−Mo-2-S micelles filled with MoS_2 nanoparticles. One can see that, in this case, individual micelles are of about 25-nm diam but tend to form loose and irregular micellar aggregates of at least 50 nm. The micelle radius value of 62 nm obtained from turbidity measurements (Table 3) shows that aggregation exists in solution as well. Here MoS_2 nanoparticles are larger than in PS-*b*-PB micelles and measure up to 4.5 nm in diameter. At the same time, the XRD profile of this sample shows no signals of MoS_2 crystallites, suggesting that MoS_2 nanoparticles are amorphous. A specific partial volume $\bar{v}$ for this sample is 0.910, demonstrating very low density of the micellar structures. For UV-irradiated PS-*b*-PIB, $\bar{v}$ is 0.919, thus, a short core-forming block of this block copolymer causes formation of low-density micellar structures independently of the presence of Mo sulfide.

(67) Khoklov, A. R.; Phillippova, O. E.; Sitnikova, N. L.; Starodubtsev, S. G. *Faraday Discuss.* **1995**, *101*, 125.
(68) Klok, H.-A.; Rebrov, E. A.; Muzafarov, A. M.; Michelberger, W.; Möller, M. *J. Polym. Sci. B: Polym. Phys.* **1999**, *37*, 485.
(69) Abes, J. I.; Cohen, R. E.; Ross, C. A. *Chem. Mater.* **2003**, *15*, 1125.

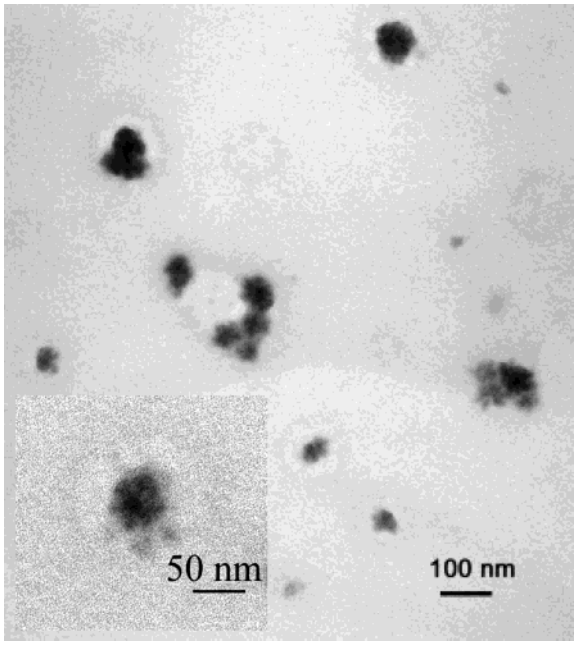

Figure 6. TEM image of PS-*b*-PIB−Mo-2-S micelles. Inset shows a higher magnification image.

Table 4. Antifrictional Properties of Mineral Oils Containing MoS_x-filled Block Copolymer Micelles[a]

sample notation	Mo content, wt. %	measurement temp., °C	critical load L_c, N	friction coefficient at L_c
mineral oil	-	20	50	0.13
PS-*b*-PB−Mo-1-S	2.5	20	350	0.08
PS-*b*-PB−Mo-1-S	2.5	90	350	0.07
PS-*b*-PB−Mo-1-S-98	2.5	20	350	0.08
PS-*b*-PB−Mo-6-S	1.8	20	550	0.07
PS-*b*-PB−Mo-8-S	3.8	20	350	0.07
PS-*b*-PB−Mo-8-S	3.8	90	250	0.08
PS-*b*-PIB−Mo-2-S	3.5	20	350	0.06
PS-*b*-PIB−Mo-2-S	3.5	90	600[b]	0.07
MoDTC[c]	12.3	90	600[b]	0.06

[a] Each sample contains 500 ppm Mo. [b] No critical load was achieved. [c] Mo 2-ethylhexyldithiocarbamate.

Tribological Properties of MoS_x-Filled PS-*b*-PB and PS-*b*-PIB Micelles. Results of tribological tests, i.e., values of friction coefficients at the critical load at 20 and 90 °C, are shown in Table 4. The lower the friction coefficient, the better the antifrictional properties. As can be seen, all MoS_x-containing block copolymer samples show reasonably low friction coefficients, the values of which are comparable to that of Mo dithiocarbamate (an efficient antifriction modifier).[25] At the same time, the important tribological parameter is the critical load, L_c, i.e., the value of a load allowing one to get the lowest value of the friction coefficient (at the load higher than L_c, the friction coefficient dramatically increases). From the data presented in Table 4, one can see that for PS-*b*-PB−Mo-1-S containing MoS_x species in the micelle core, L_c is smaller than that for PS-*b*-PB−Mo-6-S containing MoS_x nanoparticles in the micelle corona. Apparently, accessibility of the molybdenum sulfide species is a crucial factor for improvement of antifrictional properties. When MoS_x nanoparticles are located in the micelle corona, they can be easily delivered to the working surface, whereas location of molybdenum sulfide species in the core (as in the case of PS-*b*-PB−Mo-1-S) makes this task more difficult. Increase of examination temperature to 90 °C, becoming close to the glass transition temperature (T_g) of PS,[70] should result in partial softening of the micelle core and better access to the MoS_x species located there. Indeed, this leads to a lower friction coefficient, although L_c does not change. In addition, comparison of the PS-*b*-PB−Mo-1-S and PS-*b*-PB−Mo-1-S-98 samples shows that the MoS_x nanoparticle composition (MoS vs MoS_3, respectively) does not influence the antifrictional properties.

For PS-*b*-PIB−Mo-2-S, containing MoS_2 nanoparticles in the small PS core, the temperature influence is even more evident: although at 90 °C the friction coefficient increases slightly, but a load value of 600 N (limiting for the instrument used) is not a critical load. In fact, a critical load is not reached similar to Mo 2-ethylhexyldithiocarbamate (MoDTC, Table 4). Apparently, for a short PS block, T_g is lower[65] so 90 °C affords complete softening the core. In addition, PS-*b*-PIB micelles are small and very loose (see discussion above) so micelle deformation and availability of the particles located in the core should be much higher and quite satisfactory even at room temperature. At the same time, when MoS_x species are located in the micelle corona, an increase of working temperature does not improve antifrictional properties (PS-*b*-PB−Mo-8-S): the friction coefficient increases and the critical load decreases. Obviously, at 20 °C the PB block is already above T_g while a higher testing temperature can cause undesirable changes (cross-linking) in the PB corona containing MoS_x species.

Another important observation can be derived from the comparison of PS-*b*-PB−Mo-6-S and PS-*b*-PB−Mo-8-S samples. Increase of Mo content in micelle corona leads to an increase of the friction coefficient and a decrease of the L_c. This seems to be counterintuitive, as the amount of species improving antifrictional properties increases. However, analysis of the TEM images of these samples shows that the size of discrete PS-*b*-PB−Mo-6-S micelles is about 40 nm (Figure 4b), whereas PS-*b*-PB−Mo-8-S micelles measure 70−85 nm in diameter (figure is not shown). Increase of the micelle size with increase of Mo content in the corona can be caused by formation of compound micelles (or well-defined micellar aggregates) when coronas interact with each other. Apparently, larger coronas lead to inferior access to the MoS_x species (compared to smaller ones) and worsened antifrictional properties.

Because for PS-*b*-PIB−Mo-2-S we observe the highest critical load, which is higher than the one for PS-*b*-PB−Mo-6-S (where MoS_x nanoparticles are located in the micelle corona), we think that not *only* the nanoparticle availability, but also the particle size, is important to provide enhanced antifrictional properties. In PS-*b*-PIB−Mo-2-S, MoS_2 nanoparticle size is about 4.5 nm, whereas in other samples nanoparticles do not exceed 2-nm diameter or even below 1 nm (in PS-*b*-PB−Mo-6-S). One might speculate that it should be an optimal MoS_x particle size ensuring the best tribological performance, but so far we cannot make this conclusion. In our furture work we plan to vary the size of MoS_2 nanoparticles formed in PS-*b*-PIB micelles and to study

(70) Mark, H. F.; Bikales, N. M.; Overberger, C. G.; Menges, G.; Kroschwitz, J. I., Eds. *Encyclopedia of Polymer Science and Engineering*; John Wiley & Sons: New York, 1989; Vol. 16.

Table 5. Antiwear Characteristics of Mo-Containing Samples

additive in mineral oil	additive concn wt %	Mo content ppm	wear index, D_w mm
no additive[a]			0.63
PS-*b*-PIB[a]	2.3		0.63
PS-*b*-PIB−Mo-2-S[a]	2.3	500	0.39
$[(iso\text{-}C_8H_{17})_2NCS_2]_2MoOS$[71]	1	1300	0.47
$[(n\text{-}C_4H_9)_2NCS_2]_2Mo_2S_4$[71]	2	5400	0.40

[a] Experimental conditions: time of 3600 c, load of 196 N.

correlation between the particle size and tribological properties, as this paper focuses on other aspects of synthesis and properties of block copolymer micelles with MoS_x nanoparticles.

For PS-*b*-PIB and PS-*b*-PIB−Mo-2-S samples, we examined antiwear properties (Table 5). Incorporation of PS-*b*-PIB does not change the wear index (the diameter of the wear spot), but addition of PS-*b*-PIB−Mo-2-S, providing only 500 ppm of Mo, results in significant improvement: antiwear index decreases. It is noteworthy that two Mo dithiocarbamates traditionally used as antifriction and antiwear additives show higher or similar antiwear indexes only at much higher Mo content.[71]

Although the friction coefficients of MoS_x-filled block copolymer micelles are not lower than those of MoDTC (Table 4), the presence of PB or PIB chains makes such lubricating oils very promising for higher antiwear stability. Previously, the addition of antiwear modifiers such as PIB and other polymers resulted in significant loss of antifrictional properties.[21] In our case, low friction coefficients are achieved in the presence of polymeric antiwear modifiers. In addition, the tribological behavior remains the same after prolonged time: the tribological tests for PS-*b*-PB−Mo-6-S were repeated after 9 months and no changes in antifriction properties were observed.

(71) Zaimovskaya, T. A.; Lozovoi, Y. A.; Kuz'mina, G. N.; Parenago, O. P. *Petrol. Chem.* **1995**, *35*, 347.

Conclusion

MoS_x-filled block copolymers micelles (miscible with mineral oil) were synthesized using PS-*b*-PB and PS-*b*-PIB micelles and studied using FTIR, elemental analysis, SLS, turbidimetry, XRD, and TEM. To place MoS_x species in the PS micelle core, complexation with $Mo(CO)_6$ should be carried out in an argon atmosphere. This facilitates formation of arene $Mo(CO)_3$ complexes in the PS block. To situate MoS_x nanoparticles in the PB corona, complexation with $Mo(CO)_6$ should be carried out in a CO atmosphere. The latter suppresses formation of arene $Mo(CO)_3$ complexes and ensures olefin $Mo(CO)_x$ complexes in the PB block. MoS_x composition can be influenced by varying the sulfiding temperature. Increase of sulfiding temperature to 98 °C results in the species whose elemental analysis matches that of MoS_3 or MoS_2. For all compositions, MoS_x nanoparticles are amorphous even when nanoparticle diameter reaches 4.5 nm.

Location of MoS_x species in the micelle corona makes them more accessible to working surfaces and allows better antifrictional properties than when MoS_x species are situated in the micelle core. However, if overall micelle density is low (for PS-*b*-PIB), location of MoS_x nanoparticles in the micelle core also leads to a low friction coefficient and a high critical load. On top of that, addition of block copolymer micelles filled with MoS_x nanoparticles improves antiwear properties. This combined effect makes these micelles prospective additives to lubricating oils.

Acknowledgment. The present work was supported by ISTS grant 1577, Crompton Corp., and Russian Science Foundation for Basic Research (grants 01-03-32937 and 02-03-32613). We thank Prof. Dr. Markus Antonietti for the gift of PS-*b*-PB block copolymer and Prof. Alexei Khokhlov for fruitful discussions.

CM040147F